



HAL
open science

Ir-Na Cooperativity Controls the Diastereoselectivity of Borrowing Hydrogen C-C Alkylation on Isosorbide: Synthesis Methodology and Mechanistic Investigation

Jordan François, Jordan Rio, Erwann Jeanneau, Marie-Ève L Perrin,
Maiwenn Jacolot, Pierre- Adrien Payard, Florence Popowycz

► **To cite this version:**

Jordan François, Jordan Rio, Erwann Jeanneau, Marie-Ève L Perrin, Maiwenn Jacolot, et al.. Ir-Na Cooperativity Controls the Diastereoselectivity of Borrowing Hydrogen C-C Alkylation on Isosorbide: Synthesis Methodology and Mechanistic Investigation. *Organic Chemistry Frontiers*, 2023, 10 (19), pp.4732-4739. 10.1039/D3QO00700F . hal-04285559

HAL Id: hal-04285559

<https://hal.science/hal-04285559v1>

Submitted on 14 Nov 2023

HAL is a multi-disciplinary open access archive for the deposit and dissemination of scientific research documents, whether they are published or not. The documents may come from teaching and research institutions in France or abroad, or from public or private research centers.

L'archive ouverte pluridisciplinaire **HAL**, est destinée au dépôt et à la diffusion de documents scientifiques de niveau recherche, publiés ou non, émanant des établissements d'enseignement et de recherche français ou étrangers, des laboratoires publics ou privés.

Ir-Na Cooperativity Controls the Diastereoselectivity of Borrowing Hydrogen C-C Alkylation on Isosorbide: Synthesis Methodology and Mechanistic Investigation

Received 00th January 20xx,
Accepted 00th January 20xx

DOI: 10.1039/x0xx00000x

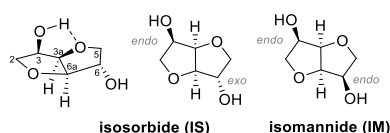
Jordan François,^a Jordan Rio,^a Erwann Jeanneau,^b Marie-Ève L. Perrin,^a Maiwenn Jacolot,^{a*} Pierre-Adrien Payard,^{a*} Florence Popowycz^{a*}

The direct functionalization of isosorbide is a current challenge of biomass valorisation due to the low selectivities usually obtained. Taking advantage of our preliminary observations concerning the diastereoselective Ir-catalyzed amination of isohexides we report the first direct C-C borrowing hydrogen direct functionalisation on isosorbide. The C-C alkylation was achieved with excellent diastereocontrol using an Ir-based organometallic homogeneous catalyst. The reaction sequence involves a catalytic dehydrogenation that converts the alcohol into a reactive ketone, the *in situ* aldol condensation / crotonisation, and a catalytic dehydrogenation leading to the homologated desired product. Once the parameters that control the reaction outcome were explored and optimized, the stereoelectronic effects from which the diastereoselectivity originates from have been investigated by means of a computational mechanistic performed at the DFT level. The roles played by the Na counter-cation to coordinate substrate's oxygen atoms and to guide hydride addition were evidenced allowing to rationalize the experimental selectivity at the molecular level.

Introduction

During the last decades, an effort has been made in order to promote the use of biobased feedstock instead of fossil resources.^{1,2} Generally, they are constituted of carbohydrate products and give directly access to high-value products for a wide range of applications in fine chemistry.³ Among them, isosorbide, a major product of the starch industry^{4,5} has received particular attention by its use as a pharmaceutical product (e.g. isosorbide dinitrate: Isordil®) or as a solvent for cosmetic applications (e.g. dimethylisosorbide).⁶ Conversion of isosorbide to high value added molecules has also attracted considerable interests both in academia and in industry for polymer applications^{7–9} and for chiral induction purposes (chiral ligand, organocatalyst or auxiliaries).^{10,11}

Figure 1. Chemical structure of isohexides



Isosorbide is a chiral molecule featuring two secondary alcohols in C-3 *endo* and C-6 *exo* positions (Figure 1). Despite the expected difference between both hydroxyl groups, the reactivity balance between both positions is currently less-pronounced in practical, leading to limited selectivities in direct transformations.¹² Thus, the functionalization of isosorbide derivatives often requires a prior step of protection of one of the two hydroxyl group.¹³ Although isosorbide functionalization into amines has been widely described using classical multi-steps strategies (alcohol activation by a tosylate followed by a nucleophilic substitution with an amine),¹³ greener alternatives must be considered nowadays. In this context, *N*-alkylation of ammonia with isohexides using the borrowing hydrogen (BH) methodology was successively reported by Beller,¹⁴ Vogt¹⁵ and Rose.¹⁶ Although these procedures are very efficient, none of them is stereoselective and they provide a mixture of three stereoisomers. To complement, we have then developed the highly diastereoselective amination of isohexide derivatives with various primary amines using a cooperative catalysis between an Ir-based complex and a Brønsted acid (Scheme 1a).^{17,18} Applying the C-C borrowing hydrogen methodology on isohexides would promote the synthesis of novel two-carbon homologated molecules that could find interesting applications in the polymer field amongst others (acids, esters and so on).

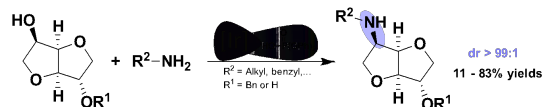
^aUniv Lyon, INSA Lyon, Université Lyon 1, CNRS, CPE Lyon, UMR 5246, ICBMS. 1 rue Victor Grignard, 69621, Villeurbanne Cedex, France

^bUniversité de Lyon, Centre de Diffractométrie Henri Longchambon, 69100 Villeurbanne, France

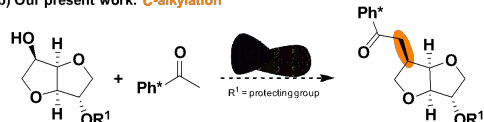
Electronic Supplementary Information (ESI) available: [details of any supplementary information available should be included here]. See DOI: 10.1039/x0xx00000x

Scheme 1. C-N and C-C functionalization on isosorbide using the BH methodology

a) Our previous work: *N*-alkylation

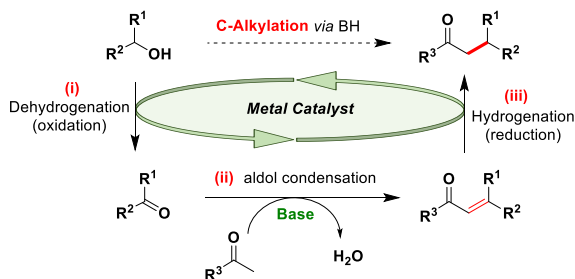


b) Our present work: *C*-alkylation



But, as far as we know, only few methodologies have been reported for the direct C-C homologation on isohexide derivatives. In 1998, Nair and coworkers reported the modification of C-6 *protected* isosorbide in a three-step sequence: oxidation of the alcohol on C-3 position, Wittig reaction and hydroboration.¹⁹ More recently, a slight variation at the C-3 position was described *via* a reaction sequence involving successively an oxidation, the Horner Wadsworth Emmons reaction and an assisted metallic reduction.²⁰ In 2011, van Es reported the double functionalization of isomannide to afford the di-carboxylic acids through triflation, nucleophilic substitution followed by hydrolysis into acid.²¹ Although effective, these syntheses have some limitations: toxicity of reagents, number of steps, low atom-economy, regio- and stereo-selective issues. The BH strategy thus appears as a promising alternative for the two-carbon elongation of isosorbide (Scheme 1b). This powerful tool indeed allows the direct activation of alcohols to form novel C-N and C-C bonds assisted by a metallic catalyst without the external use of molecular hydrogen.^{22–25} Furthermore, this one-pot strategy promotes the atom economy, the reduction of waste and the generation of a stoichiometric amount of water as sole by-product. In the case of the C-C bonds construction, the BH reaction consists in (i) a catalytic dehydrogenation that converts the secondary alcohol into a more reactive ketone, (ii) the *in situ* aldol condensation with a α -methyl ketone giving the corresponding α,β -unsaturated ketone, (iii) a catalytic dehydrogenation leading to the C-alkylated awaited compound (Scheme 2).

Scheme 2. General BH principle for the α -alkylation of ketones



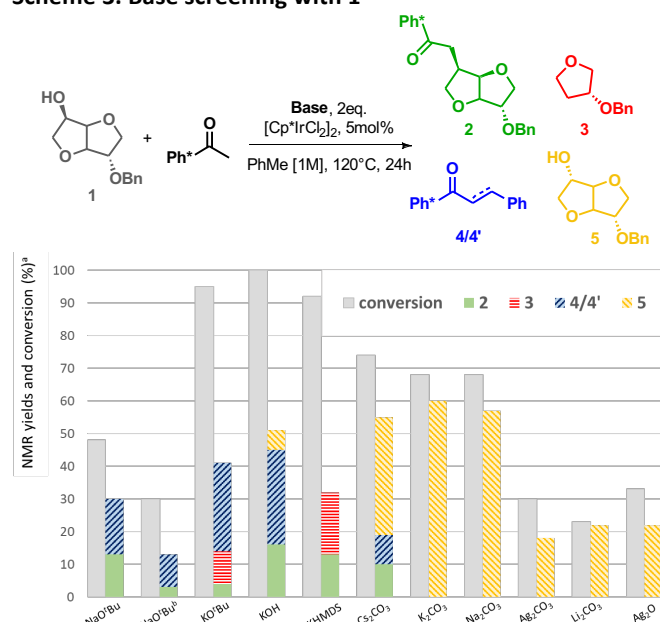
The choice of the nucleophile was crucial for the exploration of this reaction. In 2017, Donohoe's group described the synthesis of α -alkylated ketones using secondary alcohols and pentamethylacetophenone (Ph*-methyl ketone).²⁶ Advantages of the Ph*-methyl ketone are multiple: it avoids self-

condensation due to its steric hindrance, and the Ph* moiety can then be displaced *via* a retro Friedel-Crafts reaction to ultimately obtain the corresponding acid, ester, amide or alcohol.^{27,28} Capitalizing on the success of Donohoe's group in the use of Ph*-methyl ketone as an ester (or acid or alcohol) surrogate, we envisioned to extend the C-C borrowing hydrogen methodology to the non-trivial isosorbide case.

Results and discussion

This study began by performing BH reaction with pentamethylacetophenone (1.1 eq.) and commercially available isosorbide (1.0 eq.) under Donohoe's classical conditions²⁶ in the presence of $[\text{Cp}^*\text{IrCl}_2]_2$ (5 mol%) ($\text{Cp}^* = \text{C}_5\text{Me}_5$) and NaO^tBu (2.0 eq.) in PhMe at 120 °C for 24 hours. Contrary to the conditions used commonly (2 eq. of primary or secondary alcohol), the use of only 1 eq. of isosorbide was another challenge to better valorize this biosourced alcohol. Despite a complete conversion (96%), the desired product was not detected. We presumed that isosorbide undergoes degradation during the reaction leading to volatile by-products that could not be detected by NMR.^{29,30} Indeed, a difficult balance was again pointed out in between selective functionalization and degradation pathways. To decrease the functional complexity of the substrate and to understand the formation of side products, the *exo*-monobenzylated isosorbide **1** was then considered as a model substrate (Scheme 3). The choice to protect the *exo*-position was made according to previously reported calculations mentioning that the oxidation of the hydroxyl group in the *endo* position is kinetically favored by a difference in energy barriers of 2 kcal.mol⁻¹.³¹

Scheme 3. Base screening with **1**



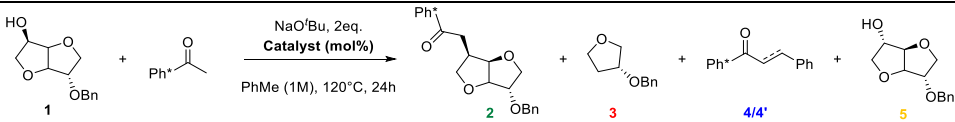
Reaction conditions: **1** (1.0 eq.), pentamethylacetophenone (1.1 eq.), $[\text{Cp}^*\text{IrCl}_2]_2$ (5 mol%), **base** (2.0 eq.), toluene [1M], 120 °C, 24 h.; ¹H NMR internal standard; values in parentheses indicate the yield of isolated product; ^b3 eq.

Pleasingly, when using the previously reported conditions, the expected C-C product **2** was formed but with a low yield of 13%. Noticeably, 17% of unexpected compounds **4/4'** were detected in the crude ^1H NMR (Scheme 3). The formation of **4/4'** may originate from the *in situ* formation of benzyl alcohol, raising from debenzilation of compound **1**. Increasing the amount of NaO^tBu to 3 eq. did not increase the conversion, which only reached 30% after 24 hours. Switching to KO^tBu , the conversion was improved to 95%, but generated more degradation and enhanced quantities of additional side product **3**. The isolation and characterization of the by-product **3** comforted our idea that one of the tetrahydrofuran cycles could be opened leading to volatile side-products and compound **3**. This type of degradation was already reported under acidic conditions, pointing out once again the selectivity challenge in functionalizing this substrate.^{29,32} The cutting edge issue was to find the appropriate balance between conversion and degradation / selectivity on a substrate that is difficult to handle. The use of other strong bases such as KOH or KHMSD led to the same conclusion. Switching to carbonate bases or to Ag_2O affected the conversion and only epimerized product **5** could be identified. Despite these moderate results, we decided to select NaO^tBu (2.0 eq) to pursue the methodological investigation by focusing on the screening of the catalyst (Table 1). First experiment was to run blank experiment without any catalyst (Table 1, entry 1) that led to almost complete recovery of the starting material, with only non-quantifiable traces of expected compound **2**. Based on successful α -alkylation of secondary alcohols under metal-free conditions from Morrill's group,³³ the reaction was tested without any catalyst with an

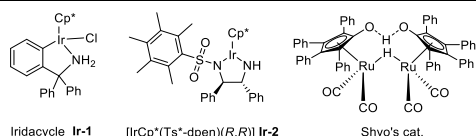
excess of alcohol (6.0 eq.): as well only traces of the expected compound were detected by ^1H NMR (Table 1, entry 2). Different iridium-based catalysts were tested with enhanced catalyst loading of up to 10 mol% (Table 1, entries 3-8). A good conversion of 77% was observed in the presence of 10 mol% of $[\text{Cp}^*(\text{Ts}^*\text{-dpen})(R,R)]$ (**Ir-2**) (Table 1, entry 7) leading to the formation of compound **2** within 30% NMR yield. Nevertheless, the side product **3** was still detected in a significant amount of 15%. When ruthenium-based catalysts (Table 1, entries 8-12) were screened, no trace of expected compound was observed, mainly compounds **4/4'** along with compound **3** were detected. Ferrocene carboxaldehyde led to complete recovery of the starting material (Table 1, entry 13). The crucial observation at this stage of the study was the observed excellent diastereoselectivity of the reaction as compound **2** was isolated as a unique diastereoisomer. Whatever the nature of the catalyst (chiral or achiral), compound **2** was formed with an excellent *dr* > 99:1. The stereochemistry of **2** was determined through ^1H NMR analysis based on the magnitude of the $\text{H}_{3'a}\text{-H}_{3'}$ coupling constant. Indeed, on the isohexide skeleton, this 3J constant that corresponds to a *cis*-coupling has a value of 4 Hz whereas the *trans*-coupling constant is around 0 to 1 Hz. $\text{H}_{3'a}$ appears as an apparent triplet considering the *cis*-coupling $J(\text{H}_{3'a}\text{-H}_{3'}) = J(\text{H}_{3'a}\text{-H}_{6'a}) = 4$ Hz, while $\text{H}_{6'a}$ turns out to be a doublet of doublet because of the lower *trans*-coupling $J(\text{H}_{6'a}\text{-H}_{6'}) = 1.2$ Hz. This observation was confirmed by NMR NOESY experiments (see SI).

Considering the large amount of by-products detected that probably results from debenzilation, we decided to prepare different mono-protected isohexides using classical methods

Table 1. Catalyst screening with 1



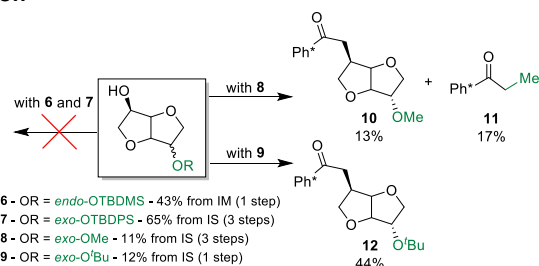
Entry	Catalyst (mol%)	Conv. (%) ^[a]	NMR yields (%) ^[a]			
			2	3	4/4'	5
1	None	traces	traces	—	—	—
2 ^[b]	None	traces	traces	—	—	—
3	$[\text{Cp}^*\text{IrCl}_2]_2$ (5)	48	13 (8%)	n.d.	17	—
4	$[\text{Cp}^*\text{IrCl}_2]_2$ (10)	44	7	n.d.	16	—
5	$[\text{Cp}^*\text{IrI}_2]_2$ (5)	26	—	n.d.	14/11	—
6	Ir-1 (10)	67	30 (30%)	n.d.	n.d./6	9 (12%)
7	Ir-2 (10)	77	30 (18%)	15	n.d.	4
8	$[\text{RuH}_2(\text{CO})(\text{PPh}_3)_3]$ (10)	33	—	n.d.	10/12	—
9	$[\text{RuHCl}(\text{CO})(\text{PPh}_3)_3]$ (10)	53	—	n.d.	18/15	—
10	$[\text{Ru}(p\text{-cymene})\text{Cl}_2]_2$ (5)	59	—	n.d.	28	n.d.
11	Shvo's catalyst (5)	0	—	—	—	—
12	$\text{RuCl}_2(\text{DMSO})_4$ (10)	100	—	—	—	—
13	Ferrocenecarboxaldehyde (10)	0	—	—	—	—



Reaction conditions: **1** (1.0 eq.), pentamethylacetophenone (1.1 eq.), catalyst (mol%), NaO^tBu (2.0 eq), toluene [1M], 120 °C, 24 h. ^a1,3,5-trimethoxybenzene as ^1H NMR internal standard; values in parentheses indicate the yield of isolated product, ^b6 eq of **1**

(see SI) such as silanes ethers (**6** and **7**) or alkyl ethers (**8** and **9**) (Scheme 4). Compounds **7**, **8** and **9** were synthesized from isosorbide while compound **6** was prepared from isomannide.

Scheme 4. Mono-protected isohexides submitted to BH reaction



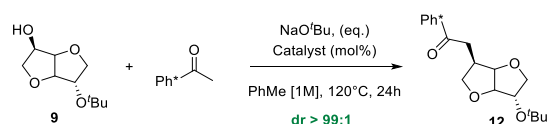
Reaction conditions (Table 1, entry 7): mono protected isohexide **6**, **7** or **9** (1.0 eq.), pentamethylacetophenone (1.1 eq.), [Cp*Ir(Ts*-dpen)(*R,R*)] (10 mol%), NaO^tBu (2.0 eq), toluene [1M], 120 °C, 24 h. ¹H NMR yields using 1,3,5-trimethoxybenzene as internal standard. TBDMS = *tert*-butyldimethylsilyl

The assessment of the influence of different protecting groups on the yield could help us (i) to understand the limitations encountered in isolating the compound of interest in high yield, (ii) to compare the influence of the *exo*-position in these two substrates. At this stage, the objective was twofold by trying to avoid by-products resulting from debenzoylation process and to increase the selectivity in favour of the C-C borrowing hydrogen product. Nevertheless, the silane derivatives **6** and **7** led to complete degradation and/or deprotection. Ether **8** reacted similarly to compound **2**, giving the expected compound **10** in a 13% NMR yield along with 1-(pentamethylphenyl)propanone **11** (17%) coming from the release of methanol in the reaction medium. In turn, ether **9** appeared as an interesting candidate because no such side product could be formed due to the quaternary carbon avoiding proton abstraction. Using the reaction conditions previously developed, the yield of C-C adduct **12** was evaluated around 40%, without any trace of side products (Scheme 4).

Further optimization of the reaction conditions was then considered starting from substrate **9** (Table 2). Cp*Ir(Ts*-dpen)(*R,R*) (**Ir-2**) appeared as the best catalyst for this transformation as other iridium catalysts (iridium dimer [Cp*IrCl₂]₂ or iridacycle **Ir-2**) led to the formation of the desired product with only 11% and 14% yield respectively (Table 2, entries 3-4). Pleasingly, we could decrease the amount of base to 1 eq. without any loss of reactivity (Table 2, entry 5). Also, when decreasing the catalyst loading to 5 or even 2 mol%, compound **12** could be isolated within similar yields (Table 2, entries 6 and 7). Time and temperature parameters were also investigated without any improvement (Table 2, entries 8-10). The best conditions were thus determined to be 2-5 mol% of iridium catalyst **Ir-2** and 1.0 eq. of NaO^tBu giving **12** with a correct isolated yield of 47% (Table 2, entry 7). Even when increasing the amount of isosorbide derivative to 2.0 eq., the yield of the reaction did not exceed 50% (Table 2, entry 11).

Applying Donohoe's conditions to isosorbide scaffolds proved to be quite challenging to reach high yields relative to simple substrates, but the perfect stereo-controlled C-C functionalization on isosorbide derivative is remarkable. As previously mentioned, a plausible pathway for this reaction,

Table 2. Optimization with 9



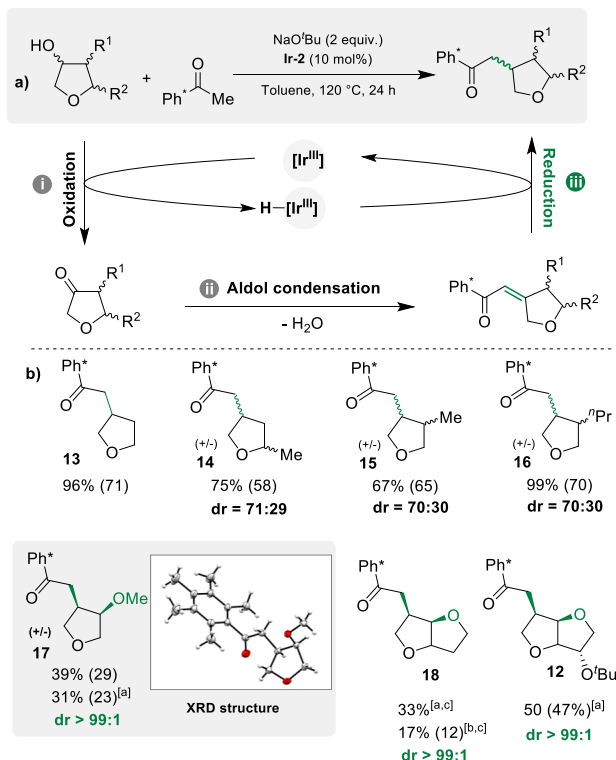
Entry	Cat. (mol%)	eq base	Conv. 9 (%) ^[a]	Yield 10 (%) ^[a]
1 ^[b]	Ir-2 (10)	2	77	30 (18%)
2	Ir-2 (10)	2	100	44 (38%)
3	[Cp*IrCl ₂] ₂ (5)	2	94	11
4	Ir-1 (10)	2	100	14
5	Ir-2 (10)	1	100	41 (41%)
6	Ir-2 (5)	1	100	51 (37%)
7	Ir-2 (2)	1	82	50 (47%)
8 ^[c]	Ir-2 (5)	1	100	43 (40%)
9 ^[d]	Ir-2 (5)	1	26	17
10 ^[c,d]	Ir-2 (5)	1	77	40
11 ^[e]	Ir-2 (2)	1	47	47

Reaction conditions: **9** (1.0 eq.), pentamethylacetophenone (1.1 eq.), **catalyst** (mol%), NaO^tBu (eq), toluene [1M], 120 °C, 24 h. ^a1,3,5-trimethoxybenzene as ¹H NMR internal standard; values in parentheses indicate the yield of isolated product, ^breaction performed with **1**, ^c48 h, ^d100 °C, ^e2 eq. of **9** (conversion based on Ph*-methyl ketone)

that does not involve change in oxidation state of the metal, would successively consist in (i) oxidation of the alcohol into ketone *via* a Ir(III)-catalysed dehydration, (ii) aldol condensation and (iii) enol reduction *via* hydrogenation (Scheme 5a). However, numerous previous mechanistic studies and reviews highlighted the diversity of factors such as catalyst, ligand, additives and / or solvent that control the reaction and its selectivity, making each catalytic system mechanistically unique.³⁴⁻⁴⁰ To evidence the factors that guide the stereoselectivity under our reaction conditions, a combined experimental and theoretical mechanistic investigation was conducted. First, the role of the structure of the isohexide was experimentally addressed through a deconvolution strategy. Simplified substrates were tested to understand how the reactivity and selectivity were impacted by the steric hindrance and the functionalization of the substrate (Scheme 5b). 3-Hydroxytetrahydrofuran was first engaged in BH reaction using 5 mol% of iridium catalyst **Ir-2** affording the expected compound **13** within excellent yield (96% NMR yield and 71% isolated yield), showing the robustness of the method. Adding a methyl group, either in β or α position led to compounds **14** and **15** with comparable yields (75 and 67% yield respectively). However, independently of the position of the methyl group, a moderate *dr* of 70:30 was measured, thus highlighting the importance of the coordinating group towards the selectivity of the reaction. A very similar trend was observed when replacing the methyl with a ⁿPr group: compound **16** was obtained in 70% yield and with a moderate *dr* of 70:30. On the contrary, the presence of a methoxy group in α position gave **17** in

significantly lower amounts (30-40%, using either 1.0 or 2.0 eq. of base), but we were delighted to observe an enhanced *dr* of 99:1. The structure of **17** was confirmed by solid-state X-ray diffraction (XRD) analysis (Scheme 5b and SI).

Scheme 5. a) General mechanism proposed for the BH C-C alkylation. b) Extension to substituted tetrahydrofurans



Reaction conditions: hydroxy-THF derivative (1.0 eq.), pentamethylacetophenone (1.1 eq.), Ir-2 (10 mol%), NaOtBu (2.0 eq.), toluene ([1M]), 120 °C, 24 h. ¹H NMR yields using 1,3,5-trimethoxybenzene as internal standard; ^a2 mol% Ir-2 and 1 eq. of NaOtBu were used; ^b10 mol% Ir-2 was used; ^cobtained along with non-reduced product (10 to 20% yield)

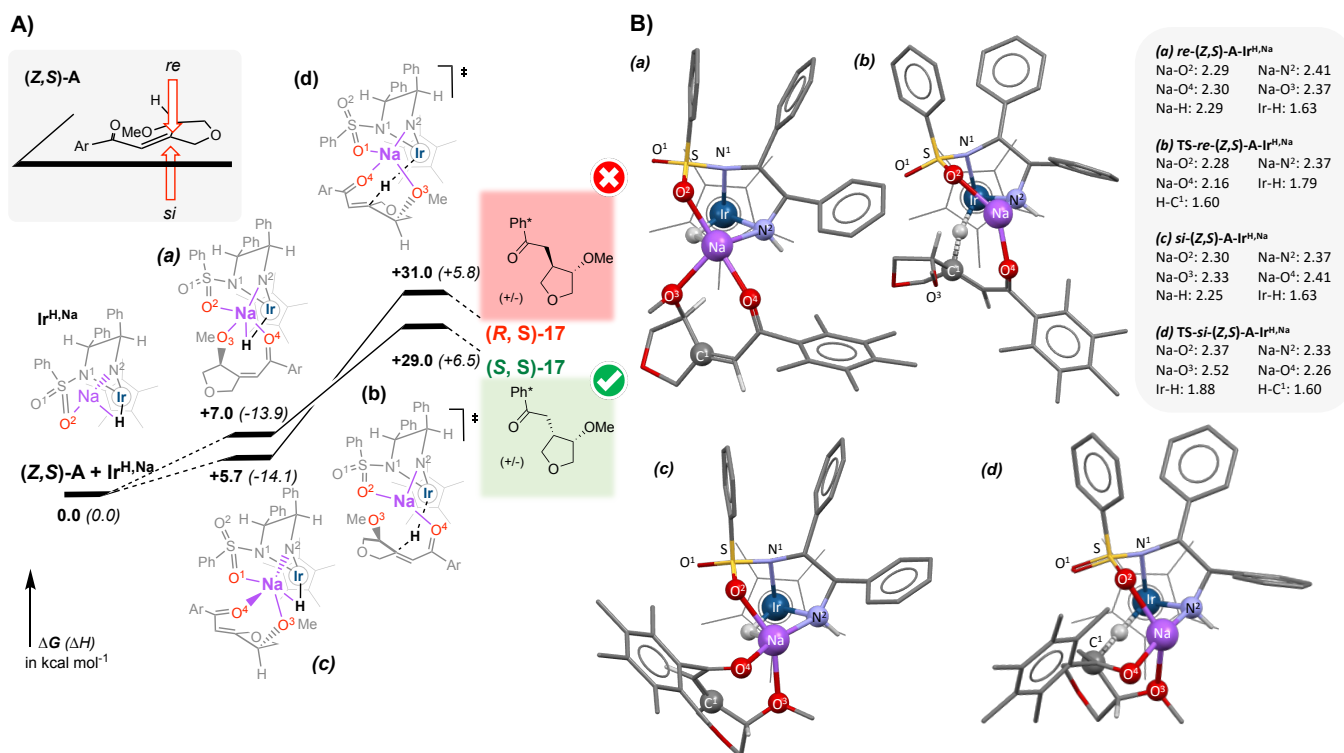
Quite similar results were obtained with mono-deoxyisorbide, but surprisingly derivative **18** was obtained along with the non-reduced adduct **18'** (see SI). The high stability of **18'** with an *endo*-cycle saturation that is obtained by isomerization of the aldol product, is assumed to prohibit its reduction by the hydride. All in all, these experimental results suggest that the presence of a heteroatom at the C-4 position of the heterocycle benefits the selectivity, while its exact role – at the molecular scale – remained unclear.

The importance of considering solvation and ion-pairing effects in *d*⁸- or *d*⁹-metal catalyzed hydrogenations reactions has been outlined by several groups.^{36–39} Since an excess of NaOtBu was used, the catalyst [Cp*Ir(Ts*-dpen)(R,R)] (Ir-2) should exist under reaction conditions in its deprotonated state [Cp*Ir(Ts*-dpen)(H)(R,R)]·Na⁺ (Ir^{Na,H}) in which the sodium counter-ion comes from the base, and the hydride arises from alcohol-to-ketone oxidation. However, the role played by the sodium cation in the stereoselectivity of the reaction must be clarified. To understand how the stereoselectivity of the reduction step (Scheme 5a, step iii) is influenced by the methoxy substituent

and the counter-cation used, a theoretical mechanistic investigation has been performed at a DFT level using the M06 functional (detailed computational procedure in SI).⁴¹ As a chemical model, the Ts*-dpen ligand has been simplified into the Ph-SO₂-dpen one by removing the Me groups of the Ph ring. This structural simplification is supported by experimental evidences as using Ts-dpen or Ph-SO₂-dpen instead of Ts*-dpen led to similar reactivity and diastereoselectivity but with a slight decrease in yield. No additional structural simplification has been done. As shown in Scheme 6, up to 8 stereoisomers of the conjugate ketone can be formed potentially by the aldol condensation and thus coexist under the reaction conditions as suggested by their relative stabilities (Scheme S1). As the reaction is not enantioselective, we have focused the mechanism investigation on the reduction of the most relevant (**Z,S**)-**A** isomer to restrict the number of substrate considered. Additional reduction mechanisms are available in SI (Schemes S3-S5). Among the Ir-complexes that could be formed between the reagents and the precursors under the experimental conditions, the deprotonated Ir-hydride complex Ir^{Na,H} is the most stable one (detailed speciation is given in Scheme S2). Thereof, in the energy profile presented in Scheme 6, Gibbs energies are relative to the ones of Ir^{Na,H} and (**Z,S**)-**A**.

Ir^{Na,H} is an octavalent heterobimetallic Ir/Na complex in which the nitrogen atoms N¹ and N² of Ph-SO₂-dpen ligand (Scheme 6), the hydride and the Cp* ligands coordinate the Ir(III) centre. In this complex, Ir and Na are bridged by the hydride, and by the N² and O² atoms of the Ph-SO₂-dpen (Scheme 6). The reduction starts with the coordination of the catalyst Ir^{Na,H} to either the *re* or the *si* face of (**Z,S**)-**A** substrate to give adducts *re*-(**Z,S**)-**A**-Ir^{Na,H} or *si*-(**Z,S**)-**A**-Ir^{Na,H}, respectively (Scheme 6). The formation of adduct *re*-(**Z,S**)-**A**-Ir^{Na,H} is thermodynamically disfavoured by 7.0 kcal mol⁻¹. The oxygen atoms O³ of the methoxy group and O⁴ of the carbonyl groups of the complexed *re*-(**Z,S**)-**A** substrate chelates the sodium ion (Na-O³: 2.37 Å, Na-O⁴: 2.30 Å) within the plane defined by the π-system of the enone. Interestingly, the Na-H distance is not affected by the coordination of the substrate. The hydride transfer then occurs *via* transition state TS-*re*-(**Z,S**)-**A**-Ir^{Na,H} (Scheme 6b), in which the hydride is approximately at equal distance from Ir and C¹. It is worth mentioning that at transition state TS-*re*-(**Z,S**)-**A**-Ir^{Na,H}, the O³-Na interaction is lost. The overall Gibbs energy barrier for the reduction step at the *re* face is computed to 29.0 kcal mol⁻¹. The absolute configuration of the resulting product (+/-)-(**S,S**)-**17** fits with the one experimentally observed after hydrolysis. When the addition is taking place at the *si* face, the catalyst approaches directly on the side of the methoxy group. Structure of adducts *si*-(**Z,S**)-**A**-Ir^{Na,H} *re*-(**Z,S**)-**A**-Ir^{Na,H} are similar, and the pre-complex *si*-(**Z,S**)-**A**-Ir^{Na,H} is merely more stable than the *re* adduct *re*-(**Z,S**)-**A**-Ir^{Na,H} by 1.3 kcal mol⁻¹. The associated transition state for the hydride transfer TS-*si*-(**Z,S**)-**A**-Ir^{Na,H} is later than transition state TS-*re*-(**Z,S**)-**A**-Ir^{Na,H} (Scheme 6d). It requires the Ir-H bond to be more elongated by 5% and the C¹ atom more pyramidalized than in TS-*re*-(**Z,S**)-**A**-Ir^{Na,H} (see Scheme S6). This transition state leads to the formation of (+/-)-(**R,S**)-**17** product that is not observed experimentally.

Scheme 6. A) Free energy profile for hydride transfer from Ir^{H,Na} at the *re* or *si* face of (Z,S)-A and B) associated structures of adducts (a) *re*-(Z,S)-A-Ir^{H,Na} and (c) *si*-(Z,S)-A-Ir^{H,Na} and transition states (b) TS-*re*-(Z,S)-A-Ir^{H,Na} and (d) TS-*si*-(Z,S)-A-Ir^{H,Na}.



Distances are given in Å. Gibbs energies are computed at the M06 DFT level. For clarity purposes, hydrogen atoms are not displayed

The overall Gibbs energy barrier of this pathway is computed to 31.0 kcal mol⁻¹, *i.e.* 2.0 kcal mol⁻¹ higher than TS-*re*-(Z,S)-A-Ir^{H,Na}. This trend is in good agreement with the experimentally observed *dr* ratio of 99:1, as the computed $\Delta\Delta G^\ddagger$ of 2.0 kcal mol⁻¹ would correspond to a *dr* ratio of 92:8. We have then further questioned the counter-intuitive preference for the MeO-Na coordination at the face opposite to the methoxy group. Interaction-Distortion Analysis (IDA)^{42,43} reveals that the electronic energy required for substrate distortion is considerably lower when reduction occurs at the *re* face than at the *si* face (see Scheme S6). This confirms the crucial role played by the coordination of the methoxy group to Na to promote the diastereoselectivity of the reduction. All in all, the remarkable selectivity obtained for this reaction originates from the coordination of the methoxy group to the sodium cation. By favoring coordination of the substrate on its *re* face, Na favors the hydride addition to the face opposite to the methoxy group.

Conclusions

Direct or post-functionalization valorisation of isosorbide raises considerable interests both in academia and in industry. However, direct and selective functionalization of isosorbide is a challenge and most reported conditions suggest multi-steps strategies. Here we report the direct diastereoselective C-C alkylation on *exo*-protected isosorbide using pentamethylacetophenone. Protection of the *exo*-alcohol was

required. The choice of NaO^tBu as a base and the protection of the *exo*-alcohol by a ^tBu group enable us to isolate the desired product with yields up to 47% with an excellent diastereoselectivity of 99:1.

A joint experimental and computational mechanistic study revealed the crucial role played by the Ir / Na heterobimetallic hydride complex as the active complex in the observed diastereocontrol. This joint methodology of synthesis and mechanistic reasoning study, not only illustrates the challenge in valorizing straightforwardly this biosourced alcohol, but also pave the way to further direct homologation and/or functionalization of polyfunctional bio-sourced compounds.

Author Contributions

The methodology of synthesis was designed by MJ and FP. Experimental work was performed by JF and molecular modelling by JR based on preliminary calculations from JF. The interplay between experiment and theory was supervised by PAP and MELP. XRD was performed by EJ. The manuscript was collegially written by all authors.

Conflicts of interest

There are no conflicts to declare.

Acknowledgements

The authors are grateful for the access to the MS analysis at the CCSM and NMR facilities at CCRMN at the Université Lyon 1. The CCIR of ICBMS is acknowledged for providing computational resources and technical support.

Notes and references

- K. Huang, X. Peng, L. Kong, W. Wu, Y. Chen and C. T. Maravelias, *ACS Sustain. Chem. Eng.*, 2021, **9**, 14480–14487.
- Y. Queneau and B. Han, *The Innovation*, 2022, **3**, 100184.
- J. J. Bozell and G. R. Petersen, *Green Chem.*, 2010, **12**, 539–554.
- G. Flèche and M. Huchette, *Starch - Stärke*, 1986, **38**, 26–30.
- C. Dusseigne, T. Delaunay, V. Wiatz, H. Wyart, I. Suisse and M. Sauthier, *Green Chem.*, 2017, **19**, 5332–5344.
- R. Seemayer, N. Bar and M. P. Schneider, *Tetrahedron Asymmetry*, 1992, **3**, 1123–1126.
- M. Rose and R. Palkovits, *ChemSusChem*, 2012, **5**, 167–176.
- F. Fenouillot, A. Rousseau, G. Colomines, R. Saint-Loup and J.-P. Pascault, *Prog. Polym. Sci.*, 2010, **35**, 578–622.
- D. J. Saxon, A. M. Luke, H. Sajjad, W. B. Tolman and T. M. Reineke, *Prog. Polym. Sci.*, 2020, **101**, 101196.
- M. Janvier, S. Moebis-Sanchez and F. Popowycz, *Eur. J. Org. Chem.*, 2016, **2016**, 2308–2318.
- M. Kadraoui, T. Maunoury, Z. Derriche, S. Guillarme and C. Saluzzo, *Eur. J. Org. Chem.*, 2015, **2015**, 441–457.
- D. Abenhaim, A. Loupy, L. Munnier, R. Tamion, F. Marsais and G. Quéguiner, *Carbohydr. Res.*, 1994, **261**, 255–266.
- M. Janvier, S. Moebis-Sanchez and F. Popowycz, *CHIMIA*, 2016, **70**, 77.
- S. Bähn, S. Imm, L. Neubert, M. Zhang, H. Neumann and M. Beller, *ChemCatChem*, 2011, **3**, 1853–1864.
- D. Pinggen, O. Diebolt and D. Vogt, *ChemCatChem*, 2013, **5**, 2905–2912.
- R. Pfützenreuter and M. Rose, *ChemCatChem*, 2016, **8**, 251–255.
- M. Jacolot, S. Moebis-Sanchez and F. Popowycz, *J. Org. Chem.*, 2018, **83**, 9456–9463.
- F. Bahé, L. Grand, E. Cartier, M. Jacolot, S. Moebis-Sanchez, D. Portinha, E. Fleury and F. Popowycz, *Eur. J. Org. Chem.*, 2020, 599–608.
- Q. Chao, J. Zhang, L. Pickering, T. S. Jahnke and V. Nair, *Tetrahedron*, 1998, **54**, 3113–3124.
- J. M. Apgar, A. Arasappan, T. Biftu, P. Chen, D. Feng, E. Guidry, J. Hicks, A. Kekec, K. Leavitt, B. Li, T. Mccracken, I. Sebhat, X. Qian, L. Wei, R. Wilkening, Z. Wu, WO2014031515A1, 2014; Merck Sharp & Dohme.
- J. Wu, P. Eduard, S. Thiyagarajan, J. van Haveren, D. S. van Es, C. E. Koning, M. Lutz and C. Fonseca Guerra, *ChemSusChem*, 2011, **4**, 599–603.
- M. H. S. A. Hamid, P. A. Slatford and J. M. J. Williams, *Adv. Synth. Catal.*, 2007, **349**, 1555–1575.
- A. J. A. Watson and J. M. J. Williams, *Science*, 2010, **329**, 635–636.
- A. Corma, J. Navas and M. J. Sabater, *Chem. Rev.*, 2018, **118**, 1410–1459.
- A. Quintard and J. Rodriguez, *Chem. Commun.*, 2016, **52**, 10456–10473.
- W. M. Akhtar, C. B. Cheong, J. R. Frost, K. E. Christensen, N. G. Stevenson and T. J. Donohoe, *J. Am. Chem. Soc.*, 2017, **139**, 2577–2580.
- C. B. Cheong, J. R. Frost and T. J. Donohoe, *Synlett*, 2020, **31**, 1828–1832.
- J. R. Frost, C. B. Cheong, W. M. Akhtar, D. F. J. Caputo, K. E. Christensen, N. G. Stevenson and T. J. Donohoe, *Tetrahedron*, 2021, **86**, 132051.
- Y. Wang, J. Wu, C. E. Koning and H. Wang, *Green Chem.*, 2022, **24**, 8637–8670.
- D. Horton, *Advances in Carbohydrate Chemistry and Biochemistry*, Academic Press, 1992, vol. 49.
- J. Gross, K. Tauber, M. Fuchs, N. G. Schmidt, A. Rajagopalan, K. Faber, W. M. F. Fabian, J. Pfeffer, T. Haas and W. Kroutil, *Green Chem*, 2014, **16**, 2117–2121.
- C. Berini, A. Lavergne, V. Molinier, F. Capet, E. Deniau and J.-M. Aubry, *Eur. J. Org. Chem.*, 2013, 1937–1949.
- M. B. Dambatta, J. Santos, R. R. A. Bolt and L. C. Morrill, *Tetrahedron*, 2020, **76**, 131571.
- D. Balcells, A. Nova, E. Clot, D. Gnanamgari, R. H. Crabtree and O. Eisenstein, *Organometallics*, 2008, **27**, 2529–2535.
- T. Kwok, O. Hoff, R. J. Armstrong and T. J. Donohoe, *Chem. – Eur. J.*, 2020, **26**, 12912–12926.
- P. A. Dub, N. J. Henson, R. L. Martin and J. C. Gordon, *J. Am. Chem. Soc.*, 2014, **136**, 3505–3521.
- J. M. Hayes, E. Deydier, G. Ujaque, A. Lledós, R. Malacea-Kabbara, E. Manoury, S. Vincendeau and R. Poli, *ACS Catal.*, 2015, **5**, 4368–4376.
- A. Lator, S. Gaillard, A. Poater and J.-L. Renaud, *Chem. – Eur. J.*, 2018, **24**, 5770–5774.
- J. Wettergren, E. Buitrago, P. Ryberg and H. Adolfsson, *Chem. – Eur. J.*, 2009, **15**, 5709–5718.
- M. R. Kita and A. J. M. Miller, *J. Am. Chem. Soc.*, 2014, **136**, 14519–14529.
- Y. Zhao and D. G. Truhlar, *Theor. Chem. Acc.*, 2008, **120**, 215–241.
- F. M. Bickelhaupt, *J. Comput. Chem.*, 1999, **20**, 114–128.
- F. M. Bickelhaupt and K. N. Houk, *Angew. Chem. Int. Ed.*, 2017, **56**, 10070–10086.